

Supplemental Information

A theoretical framework for calibrating the depth-dependent optical scattering in layered Human skin using spatially-offset measurements

SHUQUAN XIAO,¹ YUNXU SUN,¹ MARTHA VARDAKI,^{2,3} AND WEI LIU^{1,4,*}

¹*Optical Imaging Laboratory, Harbin Institute of Technology, Shenzhen, China*

²*Department of Medical Physics, School of Health Sciences, University of Ioannina, 45110 Ioannina, Greece*

³*Institute of Chemical Biology, National Hellenic Research Foundation, 48 Vassileos Constantinou Avenue, Athens, 11635, Greece*

⁴*Quantum Science Center of Guangdong-Hongkong-Macao Greater Bay Area, Shenzhen, China*

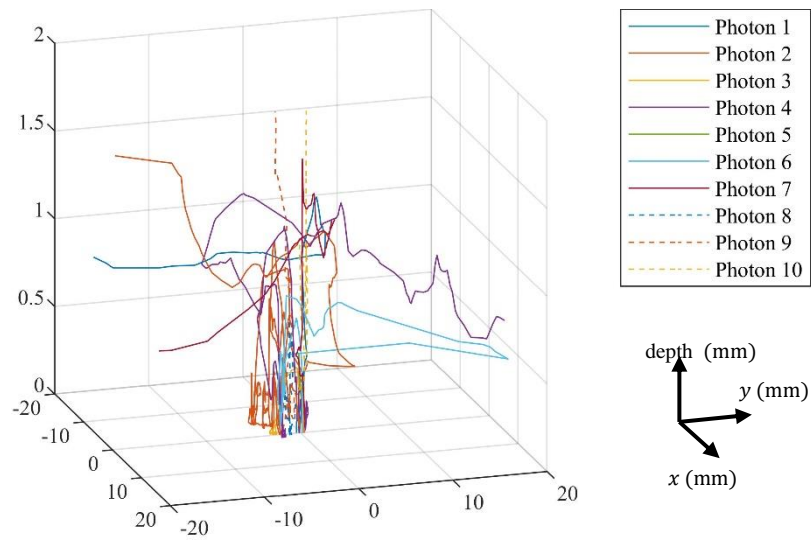
*Corresponding author: wl157@hit.edu.cn

Parameters used in Monte-Carlo simulation

Table 1.Parameters of Human skin in Monte-Carlo model

Parameters	Notation	Value
Refractive index of air	n_{air}	1.00
Refractive index of epidermis [1]	n_{ept}	1.34
Refractive index of papillary dermis [1]	n_{pap}	1.39
Refractive index of reticular dermis [1]	n_{ret}	1.40
Refractive index of subcutaneous fat [1]	n_{fat}	1.44
Wavelength (nm)	λ	800.00
Radius of the incident light (mm)	r_l	1.00
Circle radius of skin range for statistics (cm)	r_s	2.0000
Anisotropic factor [1]	g	0.852
Absorption coefficient of epidermis (mm^{-1}) [1]	$\mu_{a,ept}$	0.4104
Absorption coefficient of papillary dermis (mm^{-1}) [1]	$\mu_{a,pap}$	0.1935
Absorption coefficient of reticular dermis (mm^{-1}) [1]	$\mu_{a,ret}$	0.1575
Reduced scattering coefficient of Human skin (mm^{-1}) [2]	μ_s'	22.9730
Thickness of epidermis (mm) [3]	d_{ept}	0.10
Thickness of papillary dermis (mm) [3]	d_{pap}	0.20
Thickness of reticular dermis (mm) [3]	d_{ret}	1.57

Result Demo of the photon transportation path in Monte-Carlo simulation



Supplemental Fig. S1. Transportation path of ten normally-incident photons in Human skin.

According to the simulation steps, the transportation path of ten normally-incident photons in layered Human skin is shown in **Supplemental Fig. S1**, which becomes much more random if the penetration depth is beyond the scattering mean free path.

Accuracy Verification of NICP

Constraints in nonlinear programming:

$$\sum_{j=1}^3 A_j(S_{i1} + B_j) = MixS_i, \quad (1)$$

$$\sum_{j=1}^3 A_j(S_{i1} + B_j) \geq 0, \quad (2)$$

$$F = \prod_{k=1}^3 Grad_k, \quad (3)$$

$$Grad_k = |S_{i-1j} - A_j(S_{i1} + B_j)|, \quad (4)$$

where A is the amplification coefficient for the recovered signal, B is the bias, $Grad_k$ is the absolute difference value between the signal and the previous recovered signal, F is the objective function, i means different offsets, and j means different layers. The existences of F and $Grad_k$ help prevent the large fluctuation of the recovered signals and reduce the uncertainty.

The data sets of source signals ($Source_i$) and mixed signals (Mix_i) in accuracy verification were generated by the following equations:

$$Source_1 = 0.6\sin(32\pi x) + 0.18\sin(112\pi x) + 0.78, \quad (5)$$

$$Source_2 = 0.5\sin(24\pi x) + 0.15\sin(104\pi x) + 0.65, \quad (6)$$

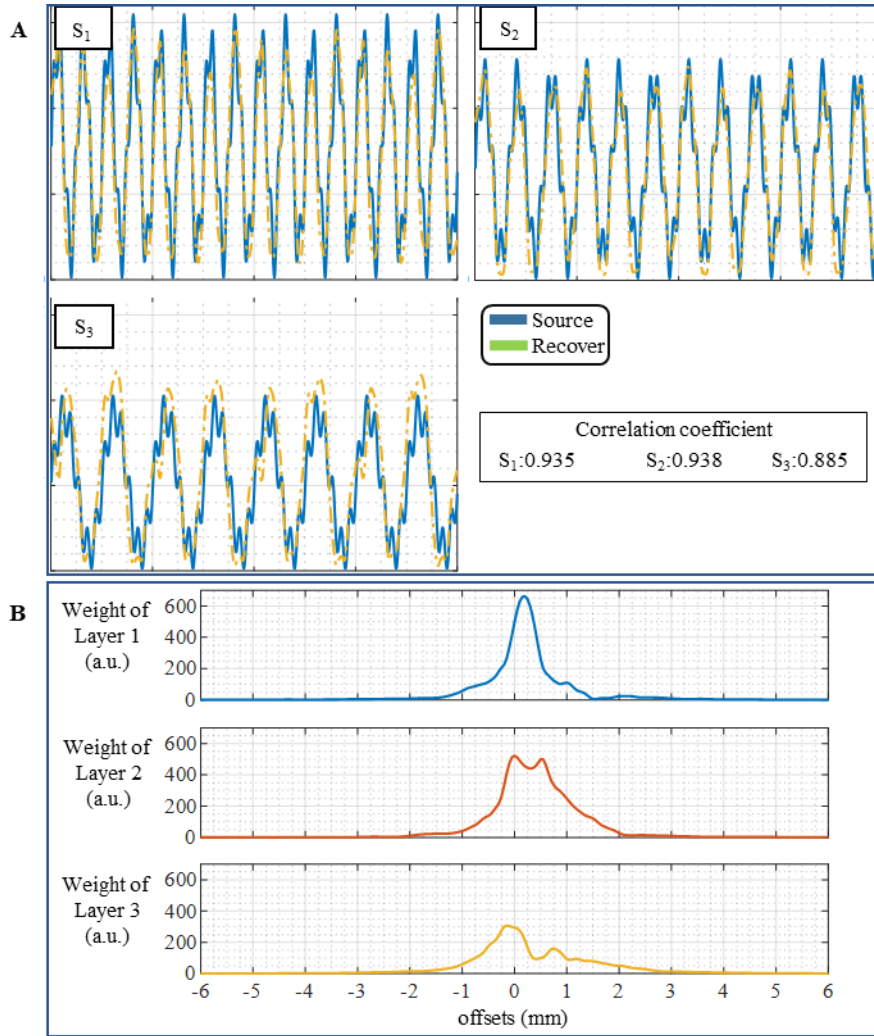
$$Source_3 = 0.4\sin(16\pi x) + 0.12\sin(96\pi x) + 0.52, \quad (7)$$

$$Mix_1 = Source_1 + Source_2 + Source_3, \quad (8)$$

$$Mix_2 = Mix_1 - R_1 Source_1, \quad (9)$$

$$Mix_3 = Mix_2 - R_2 Source_2 - (1 - R_1)R_3 Source_3, \quad (10)$$

where R_1 , R_2 , R_3 are random numbers generated in the interval $[0, 1]$. **Supplemental Fig. S2 A** clearly shows the high accuracy of NICP in recovering the source signals from the mixed data sets. By applying NICP to the total scattering photon weights, we were able to calibrate the independent contribution proportion of each layer. As shown in **Supplemental Fig. S2 B**, the three curves indicate the independent total photon weights of three layers when the incidence angle is 60 degrees, which can be used for further improving the axial resolution of SOS setups.



Supplemental Fig. S2. Applying NIPC algorithm for calibrating source signals from mixed data sets. A, test data sets, S_1 , S_2 , and S_3 indicate the three source signals (in blue) and their recoveries (in green). High recovery accuracy was obtained; B, independent depth-sensitive photon weights of each layer.

References

1. I. V. Meglinski, and S. J. Matcher, *Physiological Measurement* **23**, 741 (2002).
2. J. B. Salomatina E, Novak J, Yaroslavsky AN, *J Biomed Opt* (2006).
3. P. Oltulu, B. Ince, N. Kökbudak, S. Fındık, and F. Kılıç, *Türk Plastik, Rekonstruktif ve Estetik Cerrahi Dergisi* **26**, 56-61 (2018).